Social Neuroscience

ISSN: 1747-0919 (Print) 1747-0927 (Online) Journal homepage: www.tandfonline.com/journals/psns20

The neuronal dynamics of different types of incentives on risk-taking: comparing financial and social rewards using fMRI

Niels Doehring, Peter Erhard & Manfred Herrmann

To cite this article: Niels Doehring, Peter Erhard & Manfred Herrmann (30 Jun 2026): The neuronal dynamics of different types of incentives on risk-taking: comparing financial and social rewards using fMRI, Social Neuroscience, DOI: 10.1080/17470919.2026.2684435

To link to this article: https://doi.org/10.1080/17470919.2026.2684435

Published online: 30 Jun 2026.

SOCIAL NEUROSCIENCE
https://doi.org/10.1080/17470919.2026.2684435

Routledge
Taylor & Francis Group

RESEARCH ARTICLE

OPEN ACCESS Check for updates

The neuronal dynamics of different types of incentives on risk-taking: comparing financial and social rewards using fMRI

Niels Doehring[a,b], Peter Erhard[a] and Manfred Herrmann[a]

[a]Department of Neuropsychology and Behavioral Neurobiology, University of Bremen, Bremen, Germany; [b]Institute for Information Systems (WIN), Karlsruhe Institute of Technology, Karlsruhe, Germany

ABSTRACT

Risk-taking behavior varies across different life domains, yet neuroimaging research has primarily focused on financial incentives, thus limiting our understanding of the neural basis for domain-specific risk-taking. This study investigates whether neural correlates of risk-taking differ between financial and social incentive domains using functional magnetic resonance imaging (fMRI). Thirty-nine participants completed an adapted Balloon Analogue Risk Task with financial (monetary rewards) and social (gifts for children) incentive conditions. Behavioral data show that participants demonstrate less risk-seeking behavior in the social compared to financial condition. Neuroimaging results revealed both domain-general and domain-specific components of risk processing. A conjunction analysis of both incentive conditions identified a common neural network across both incentive types, including bilateral striatum, dorsal anterior cingulate cortex, and left insular cortex, supporting theories of domain-general risk processing mechanisms. Contrasting both reward conditions revealed significantly stronger activation in the right inferior parietal lobule during financial compared to social risk-taking, thus indicating a neural substrate for domain-specific risk preferences. These data might bridge the gap between behavioral evidence for domain-specific risk-taking and neuroimaging research, highlighting the importance of considering the type of incentives when studying risk behavior and its neural correlates.

ARTICLE HISTORY
Received 1 July 2025
Revised 30 March 2026

KEYWORDS
Risk-taking; functional magnetic resonance imaging (fMRI); social incentives; financial incentives; domain-specific risk

Introduction

Risk-taking behavior occurs in various domains of daily life, including financial investments, health-related choices, and social interactions. It has received significant attention in various research domains due to its relevance for understanding normative decision-making processes (Fischhoff & Broomell, 2020), as well as its contribution to harmful behaviors in several psychiatric conditions, including attention deficit hyperactivity disorder, bipolar disorder, and substance abuse disorders (Ashenhurst et al., 2011; Pollak et al., 2020; Reddy et al., 2014).

Several meta-analyses of functional magnetic resonance imaging (fMRI) studies have confirmed a network of brain regions involved in risk-related decision-making. This network includes, amongst others, the dorsomedial prefrontal cortex (dmPFC), the dorsal anterior cingulate cortex (dACC, cf. Clairis & Lopez-Persem, 2023), the insula, and the ventral striatum (Poudel et al., 2020; Wu et al., 2021). Within this network, the dACC is understood to be involved in monitoring and updating mental models of the current environment (Kolling et al., 2016), while the insula might play a role in affective processing during risk decisions, as also shown by lesion studies where patients with damage to the insula demonstrated diminished sensitivity to expected value in the loss domain (von Siebenthal et al., 2017). The caudate nucleus as part of the striatum is supposed to be involved in reward processing, valuation, and action selection during decision-making (Balleine et al., 2007; Lau & Glimcher, 2008; Liu et al., 2011).

Previous neuroimaging research has predominantly focused on financial or token incentives. With behavioral evidence suggesting domain specificity in risk-taking propensity, the focus on financial incentives is of only limited value with respect to everyday life situations. A systematic review by Chandrakumar et al. (2018) found no fMRI studies examining risk-taking with non-financial incentives, a finding that was also corroborated by later review studies implying financial incentives or no incentive at all besides virtual points (Poudel et al., 2020; Wu et al., 2021).

The scientific issue of domain generality versus domain specificity in risk-taking still remains under debate. The

CONTACT Niels Doehring nielsdoehring@protonmail.com Department of Neuropsychology and Behavioral Neurobiology, University of Bremen, Cognium, Hochschulring 18, Bremen D-28359, Germany

domain-specific risk-taking scale (DOSPERT; Blais & Weber, 2006) measures risk preferences across different domains and shows limited consistency across them, indicating that individuals may exhibit different risk preferences depending on the respective context of decision making. Some data, however, support a domain-general trait-like risk-taking propensity (Mata et al., 2018; Zhang et al., 2019), while others emphasize domain-specific effects (Friedl et al., 2020; Sevi & Shook, 2021; Shou et al., 2022). Nicolaou and Shane (2019) identified common genetic components accounting for an association between general and domain-specific risk-taking, while acknowledging a relevant domain-specific variance.

Several studies demonstrated an effect of the type of incentives on risk-taking behavior, using both behavioral and neuroimaging data. On the behavioral level, unpleasant odors as negative incentive decreased participants' sensitivity to the probability of losses and led to stronger deviations from optimal behavior (von Helversen et al., 2020). Similarly, non-financial rewards lead to decreased risk-taking compared to financial incentives (Rosati & Hare, 2016). On the neural level, it has been well established that rewards from different domains activate largely overlapping, but in part dissociable neural networks (Flores et al., 2015; Gu et al., 2019; Rademacher et al., 2010).

Despite behavioral evidence for incentive-dependent differences in risk-taking, the question of whether neural correlates of risk-taking depend on the incentive domain remains, to the best of the authors' knowledge, not systematically investigated. This represents a gap in the literature, as it limits the generalizability of findings from laboratory studies to real-world risk-taking situations where incentives are often of non-financial nature. Understanding the neural basis of domain specificity in risk-taking could thus improve our understanding of maladaptive risk behaviors across various contexts and could provide possible evidence of intervention strategies.

The present study tries to address this gap by comparing neural correlates of risk-taking behavior between both financial and social incentives. To achieve this goal, fMRI measurements were taken while participants completed the Balloon Analogue Risk Task (BART; Lejuez et al., 2002), an established measure of risk-taking behavior. Similarly to prior fMRI studies on the BART, a passive condition where participants did not have to make a decision but only had to press a button was introduced for contrasting (cf. Rao et al., 2008, 2018).

On a behavioral level, the study was based on the following hypothesis: Risk-taking propensity was expected to differ between social and financial incentive conditions. This hypothesis is based on established domain-specific variations in risk preferences (Blais & Weber, 2006) and further evidence that risk-taking behavior is modulated by social context (Haddad et al., 2014; Zhang et al., 2019). Due to limited prior research directly comparing these particular incentive types, the direction of this effect was not specifically predicted.

Additionally, response time differences between the different conditions were analyzed. Active trials were expected to elicit longer response times than passive trials due to additional cognitive demands of decision-making (Kyllonen & Zu, 2016). Regarding incentive type, prior literature provided insufficient basis for directional predictions. Zhang et al. (2019) found no response time differences between self- and other-directed risk-taking, but the difference between incentive types in the present study is larger compared to their design. Response time differences between incentive types were thus analyzed without specific directional hypotheses.

With respect to the neuroimaging data, we hypothesized a significant overlap of neural activation patterns between financial and social risk-taking conditions, reflecting domain-general risk processing mechanisms (Mata et al., 2018; Nicolaou & Shane, 2019) and aligned with findings on incentive-independent reward anticipation networks (Gu et al., 2019). This common network was expected to include the dACC and the dorsolateral prefrontal cortex (dlPFC), areas associated with strategy adaptation and implementation independent of the type of reward (Kolling et al., 2016; Voloh et al., 2015).

We further expected differences in neural activation patterns between incentive conditions, particularly in reward-processing regions. Based on evidence for incentive-dependent activation during reward consumption (Flores et al., 2015; Rademacher et al., 2010), the insular cortex and nucleus accumbens (NAcc) were proposed as candidate regions.

When contrasting active and passive risk-taking within each incentive condition, we expected an activation in a network similar to that identified in previous risk-taking studies (Poudel et al., 2020; Wu et al., 2021) and studies using a similar design and contrast condition (Rao et al., 2008), encompassing right dlPFC, bilateral dACC, dorsomedial prefrontal cortex, insula, striatum, and the right superior parietal lobule.

Materials and methods

Participants

The study included 39 participants (28 female, 11 male), with a mean age of 23.9 years (SD = 3.8, range 19–33 years). Participants were primarily recruited through university mailing lists, mostly from the student population

at the University of Bremen. The study was approved by the local ethics committee (approval no. 2019–14) and participants gave informed consent in accordance with the Declaration of Helsinki.

Participation was restricted to individuals between 18 and 35 years of age to control for age-related effects on risk-taking behavior and associated neural activity, which have been documented in previous research (Best & Charness, 2015). As compensation, participants received the monetary rewards accumulated during the financial incentive condition, a certificate stating the number of gift bags earned in the social condition, and students enrolled in psychology programs additionally received course credit. All participants provided written informed consent prior to participation, and the study was approved by the ethics committee of the University of Bremen.

Stimuli – the adapted Balloon Analogue Risk Task (BART)

The present study employed an adapted version of the BART designed for fMRI measurement. The BART is an established risk-taking design with demonstrated external validity (Aklin et al., 2005; Skeel et al., 2008). In this task, participants decide whether to continue inflating a virtual balloon (increasing potential reward but also increasing risk of loss) or cash out their accumulated reward. We modified this paradigm to create comparable conditions with either financial incentives (money) or social incentives (rewards benefiting others), allowing for direct comparison of neural activation patterns during risk-taking decisions across these domains.

In each trial, participants were presented with a virtual balloon that could be inflated to accumulate reward (see Figure 1). Participants were asked to imagine themselves at a funfair with an inflation machine, where they either sold balloons to adults (financial incentive) or presented them as gifts to children (social incentive). Each inflation increased the potential reward but also the probability of a balloon explosion, at which point all accumulated reward for that balloon would be lost. After each successful inflation, participants were shown the current worth of the balloon and were prompted again with the question whether they wanted to continue inflating it.

The task included both active trials, where participants made inflation decisions, and passive trials, where they observed the same stimuli but always pressed the same button and decisions were made automatically for them. This passive condition served as a control task to segregate neural activity specifically related to risk-based decision-making while controlling for reward anticipation and consumption (cf. Lei et al., 2017; Rao et al., 2008, 2018). Balloon color changed between yellow and blue depending on the condition (active/passive), with colors counterbalanced across participants.

Before the experiment started, participants were instructed about the task, and gave informed consent to participate. Questionnaires on MRI safety and demographics were completed by the participants, followed by detailed instructions on the procedure and 12 practice trials outside the scanner to ensure task understanding. After participants were positioned inside the scanner, structural T1 scans were taken prior to fMRI to familiarize participants with the scanner environment. The whole experiment duration was around 90 minutes, with the BART taking 30–35 minutes, depending on participants' responses and reaction times.

The experimental design consisted of 120 balloons in total, resulting in 30 balloons for each of the experimental conditions (social-active, social-passive, financial-active, financial-passive). Balloons could be inflated between 2 and 9 times before explosion, with an average of 5.5 inflations. The maximum balloon sizes were

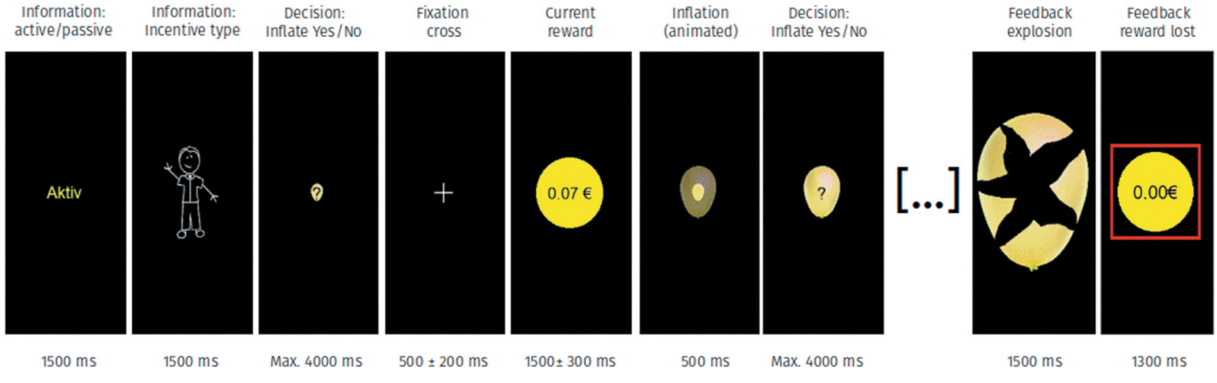

Figure 1. Experimental design showing a trial with financial incentive. Images are cropped for presentation purposes: the screen used in the pilot- and fMRI study had an aspect ratio of 4:3 Balloon trials were separated by a 3000 ms ± 1500 ms ITI.

predetermined, with an equal number of balloons bursting at each size. Passive balloon inflation stopped after 4, 5, or 6 inflations, with half of the passive balloons exploding.

The design was split into two halves with counterbalanced presentation order across participants. Trial order was pseudo-randomized but kept consistent within each counterbalancing group. The experimental session included 3 breaks – one every 30 balloons – during which the cumulative earnings from both social and financial conditions were displayed.

Each trial began with two 1.5-s instruction screens. The first screen indicated whether the upcoming balloon condition was active or passive, while in the second the incentive type was indicated using adult or child stick-figure images according to the scenario explained above. After the instruction screens, a small balloon with a question mark indicated that participants had to decide if they wanted to inflate the balloon or not. A decision to inflate was always followed by a fixation cross displayed for a randomly jittered 500 ± 200 ms period. In case the balloon exploded, an image of the broken balloon was displayed for 1500 ms, followed by "0.00€" or a neutral looking smiley face depending on the incentive condition and displayed in a red frame for 1300 ms. In case of a successful inflation, the current reward was displayed for 1500 ± 300 ms, followed by a 500 ms animation of the balloon inflating, before the question mark reappeared indicating that the next decision was expected. In case the decision was to stop inflating the balloon, amount won was displayed within a green frame, shown for 1300 ms and followed by the next trial. Trials were separated by a 3 ± 1.5 s inter trial interval (ITI; see Figure 1). An abbreviated example trial can be found in Figure 1.

Participants were asked to make their decisions within a 4-s time window. Otherwise, a screen showed "Zu langsam" (German for "too slow"), the reward for the current balloon was lost, and the next balloon trial started. Financial rewards were displayed as Euro amounts in a yellow circle, while social rewards were represented by a smiley face, with the smile being more intense as the balloon grew larger. The smiley face was chosen to make the incentives more distinct, while keeping the visual stimulus – a yellow circle with black lines – as similar as possible. Participants received monetary rewards in the financial condition, while for the social condition they were informed that gift bags containing toys would be distributed to children based on their performance. The amount of gift bags received was calculated similarly to the number of Euros, with one gift bag equaling one Euro.

Responses were communicated via button presses using the right index, middle, and ring fingers on a three-button response device, with two buttons for inflating/stopping inflation and one button for the passive condition. Button-response mapping was counterbalanced across participants. Stimuli were presented via projection onto a screen visible to participants through a mirror mounted on the head coil. The experiment was scripted in Octave (Version 4.2.1) using Psychophysics Toolbox extensions running on Ubuntu 18.04.

After the measurement, participants rated how motivating they found each incentive type on a 10-point Likert-scale.

Behavioral data analysis

Behavioral analyses were conducted in R (version 3.6.3; R Core Team, 2020) with RStudio (version 1.1.456; RStudio Team, 2016). Assumptions of normality were checked with Shapiro Wilk tests where necessary.

We calculated relative burst-scores for each participant as an estimate of risk-taking propensity (number of exploded balloons divided by total number of balloons, cf. Schmitz et al., 2016). If participants missed the response time window, the trial was omitted from analyses of risk-taking propensity. Burst scores in active trials were compared between the different incentive conditions with paired t-tests.

Differences in response times in the four conditions resulting from the two factors – trial type (active/passive) and incentive (financial/social) – were investigated using a 2 × 2 repeated measures analysis of variance (ANOVA).

fMRI scanning parameters

Functional MRI data were acquired using a Siemens Magnetom Skyra 3-Tesla scanner. Structural T1-weighted images were collected with 1 mm isometric voxel size (repetition time [TR] = 2400 ms, echo time [TE] = 2.43 ms, inversion time [TI] = 900 ms, flip angle = 8°, field of view [FOV] = 256 × 256 mm, 176 slices, 1 mm slice thickness). For functional measurements, an echo-planar imaging (EPI) sequence was employed with a GRAPPA acceleration factor of two (TE = 30 ms, TR = 2500 ms, 46 interleaved slices). The scanning was oriented parallel to the anterior and posterior commissure (AC-PC). Functional data were collected as 3 mm isometric voxels in a 64 × 64 in-slice field of view and a 3 mm slice thickness. The number of volumes varied between participants due to differences in response times and decisions, with approximately 816 volumes per participant.

fMRI pre-processing and analysis

All fMRI data analyses were conducted in AFNI (Cox, 1996; Cox & Hyde, 1997). Preprocessing began with conversion of DICOM files to NIfTI format, followed by a defacing stage to ensure participant anonymity (cf. Theyers et al., 2021). Slice timing correction was applied before estimating movement parameters using rigid-body transformations. Movement estimates were saved for use in the later analysis. Volumes with head movement exceeding 0.3 mm within a single TR were omitted from later analysis with the use of one additional regressor added to the model, to account for the full variance within the omitted volume. Alignment of functional to structural data was performed using AFNI's "lpc+ZZ" cost function (Saad et al., 2009), based on the functional volume with the minimal number of outlier voxels (+/- 3 standard deviations from average). Structural normalization was based on the MNI152-2009c template (Fonov et al., 2011). Nonlinear warping was used for structural-to-template registration. Spatial smoothing was applied using an 8 mm full-width-half-maximum Gaussian kernel. Functional data were masked based on the structural scan, and voxel-wise scaling was applied (cf. Chen et al., 2017).

For statistical analysis, a general linear model (GLM) approach was implemented. Periods of decision making, as well as positive-, and negative feedback were modeled separately for all four experimental conditions (social-active, social-passive, financial-active, financial-passive).

Decision periods preceding inflation decisions were modeled with two duration-modulated BLOCK regressors: a constant regressor for average effects and a mean-centered parametric regressor modulated by the balloon explosion probability. Feedback periods (positive and negative) were modeled with fixed-duration BLOCK regressors. Six motion parameters obtained in the motion estimation plus their derivatives were included into the GLM as nuisance regressors, along with Legendre polynomials for baseline detrending.

At the subject level, general linear tests were calculated to compare parametric regressors in active versus passive trials within each incentive type. A group-level analysis comparing the differences of active and passive risk-taking between social and financial incentives was calculated based on the subject-level results. All group-level analyses use a non-parametric cluster approach based on AFNIs 3dttest++ function. The cluster-forming threshold was set at $p < .001$, with cluster size thresholds calculated to keep false discovery rate below 5%. All tests were conducted two-sided.

Conjunction analyses were conducted to identify regions showing overlapping activation between incentive conditions. To this goal, the voxel-wise intersection of binarized statistical maps was calculated, retaining only voxels that were significant in all conditions (Nichols et al., 2005).

To establish reliability and to compare the findings with previous studies, whole-brain cluster analysis was also conducted for the contrast of parametric correlates of active and passive risk-taking within each incentive condition.

Hypotheses related to differences in activation between the incentive conditions were tested with region of interest (ROI) analyses. Extents of the regions of interest were defined using the human Brainnetome atlas (Fan et al., 2016), which parcellates the brain based on structural connectivity profiles. Atlas-based ROI definitions were chosen over meta-analytically derived coordinates for several reasons: Our hypotheses refer to activation differences at the level of anatomical structures (e.g., NAcc and insula) rather than replication of specific activation peaks from prior work, making anatomically defined regions the more appropriate operationalization. Second, for small structures such as the NAcc, spherical ROIs, whether centered on meta-analytic coordinates or the structures center of mass, risk including substantial proportions of adjacent regions (e.g., caudate nucleus, putamen), whereas atlas parcels can respect anatomical boundaries derived from structural connectivity profiles.

Within each ROI, average beta estimates were calculated for each subject and regressor of interest. The resulting values were compared in a 2 by 2 within subject ANOVA with type II sums of squares, using incentive condition and activity as factors. Values were extracted for left and right insula (Brainnetome regions 163 to 174), and the NAcc.

Results

Behavioral data analysis

The maximum response time of 4 s was exceeded in 31 of all trials (0.17%). Out of 39 participants, 27 never missed a response time interval; the highest individual omission rate was 4.6%. No participants were excluded due to missing trials.

Measures of risk-taking propensity (relative burst-scores) were compared between active trials with financial and social incentives. Burst-scores in both groups were normally distributed (W soc = .97, p soc = .44; W fin = .97, p fin = .15). A paired t-test shows significant differences between the two incentive types (t (38)=3.64,

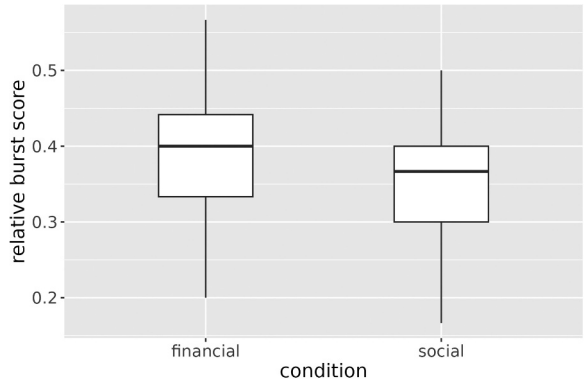

Figure 2. Relative burst scores with financial and social incentives. Relative burst scores as a measure of risk taking, indicating the percentage of exploded balloons per participant, for both incentive conditions.

$p = .001$). Participants were less risk seeking in the social incentive condition ($m = 35\%$, sd = 8% points) compared to financial incentives ($m = 39\%$, sd = 9% points). The results are illustrated in Figure 2.

Participants took on average 542 ms (sd = 384 ms) to decide. A 2×2 within subject ANOVA with the factors balloon type (active/passive) and incentive (financial/social) found a main effect of balloon type ($F(1,38) = 37.33$, $p < .001$, $\eta p 2 = .50$) and incentive ($F(1,38) = 10.82$, $p = .002$, $\eta p 2 = .22$) on the response time. No significant interaction was observed ($F(1,38) = .01$, $p = .091$). Participants took longer for active compared to passive ($m_{act} = 592$ ms, $sd_{act} = 186$ ms; $m_{pas} = 492$ ms, $sd_{pas} = 146$ ms) and social compared to financial trials ($m_{soc} = 552$ ms, $sd_{soc} = 175$ ms; $m_{fin} = 532$ ms, $sd_{fin} = 174$ ms). Data on response times are illustrated in Figure 3.

Participants self-reported how motivated they were by the different incentives after the measurement. Motivation did not differ significantly between social ($M = 7.8$, SD = 2.09) and financial ($M = 7.42$, SD = 1.92) incentives ($t(38) = 0.94$, $p = .35$).

fMRI data analysis

Risk-taking with financial incentives

Six clusters of significant differences in beta-estimates were found when contrasting active and passive risk-taking with financial incentives. For all clusters, beta-estimates were higher in the active compared to the passive condition. Clusters were located in the left striatum expanding to the left anterior insula, in the right striatum, dorsal anterior cingulate cortex (dACC), right insular cortex and bilaterally in the occipital cortex. Detailed information on cluster size, extent, and peak coordinates can be found in Table 1 and Figure 2.

Risk-taking with social incentives

Seven clusters of significant differences were found by contrasting active and passive risk-taking within the social incentive conditions. Beta-estimates were higher

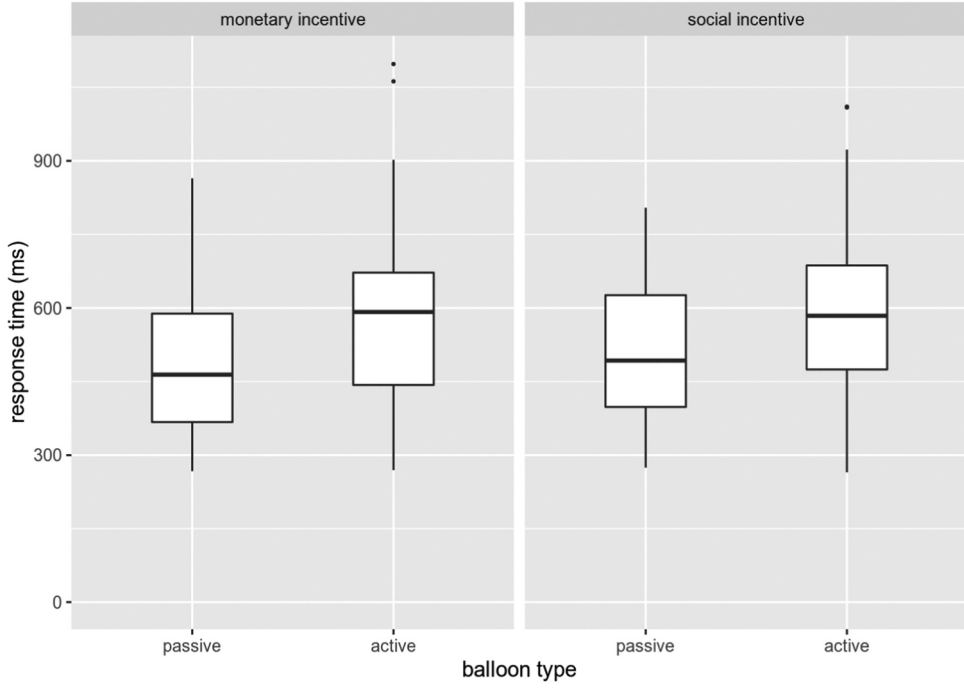

Figure 3. Boxplots of average response times in all conditions. Mean response times within each combination of conditions were calculated on the individual level.

Table 1. Results of all fMRI analyses on neural correlates of risk-taking.

Nr.	lat.	location of peak	extend	peak coordinates X	Y	Z	peak Z-score (*p*)	size voxels (mm^3)
			ea - ep minimal cluster-size for significance: 55 voxels					
			ea > ep					
1	L	orbital gyrus, <2mm from nucleus accumbens	striatum (Putamen, caudate, nucleus accumbens, globus pallidus) inferior frontal gyrus dorsal insular lobe	19.5	-4.5	-16.5	4.416(<.01)	230(6210)
2	B	dorsal anterior cingulate cortex (dACC) <2mm from medial BA9	dACC, medial and dorsolateral SFG, ACC	-1.5	-25.5	34.5	4.587 (<.01)	227 (6129)
3	B	occipital cortex	rostral cuneus, occipital cortex	-2R5.5	91.5	34.5	4.142 (<.02)	141 (3807)
4	R	putamen	striatum (putamen, caudate)	-10.5	1.5	13.5	4.211 (<.02)	111(2997)
5	L	occipital cortex (1mm: cCunG)	Left occipital cortex, caudal cuneus	1.5	103.5	4.5	4.367 (<.03)	94(2538)
6	L	dorsal agranular insula (1mm: A12/47l_right) (2mm: A44op_right)	orbital gyrus, opercular IFG, dorsal insula	-49.5	-19.5	-7.5	4.079 (<.03)	79(2133)
			ea < ep					
		No significant clusters matching criteria						
			sa – sp minimal cluster-size for significance: 57 voxels					
			sa > sp					
1	B	Medial superior occipital gyrus	occipital cortex, parietooccipital sulcus, lingual gyrus	-13.5	85.5	46.5	3.406 (<.01)	1480(39960)
2 (3)	B	dACC <1mm from subgenual ACC	dACC, medial BA9, subgenual ACC	-1.5	-37.5	19.5	3.945(<.01)	300(8100)
3 (6)	L	dorsal disgranular insula <1mm from opercular IFG < 2mm from ventral IFG < 2mm from agranular insula	striatum (Putamen, caudate, nucleus accumbens), insula, opercular IFG	43.5	-13.5	-1.5	3.834(<.01)	176(4752)
4(7)	R	nucleus accumbens	striatum (caudate, putamen, nucleus accumbens)	-16.5	-4.5	-10.5	3.292(<.02)	97(2619)
			sp > sa					
1 (2)	L	inferior parietal lobule (IPL), BA39	IPL, BA39 & BA40	34.5	76.5	52.5	-3.297(<.01)	366(9882)
2(4)	L	<3mm from inferior frontal junction	middle and inferior frontal gyrus	52.5	-22.5	40.5	-4.114(<.01)	225(6075)
3(5)	L	<2mm from orbital gyrus (A12/47l)	middle frontal, orbital and inferior frontal gyrus	49.5	-46.5	-16.5	-4.159(<.01)	213(5751)
			(ea-ep) – (sa-sp) minimal cluster size for significance: 54 voxels					
			ea-ep > sa-sp					
1	R	< 1mm from Cuneus	caudate, rostrodorsal BA39 & BA40	-49.5	52.5	58.5	4.007(<.04)	68(1647)
			ea-ep < sa-sp					
		No significant clusters matching criteria						
			ea-ep ∩ **sa-sp** conjunction of ea-ep and sa-sp, no minimal cluster size					
		Location of internal center		Center of massX				
1	B	dACC	medial BA9	-4.5	-25.5	28.5	1	B
2	R	lateral occipital cortex	occipital cortex	-13.5	88.5	22.5	2	R
3	L	ventromedial putamen <1mm from left caudate	Left striatum (caudate, putamen, anterior cingulate)	19.5	-10.5	-4.5	3	L
4	R	ventromedial putamen <1mm from right caudate	Right striatum (caudate, putamen)	-16.5	-10.5	-1.5	4	R
5	L	occipital cortex	Left occipital cortex	7.5	97.5	13.5	5	L

Note. Cluster peak location and extent. For conjunction analysis, internal center coordinates (as calculated through AFNIs iCenter function) are given. Regions accounting for less than 5% of a cluster are not included in the table. All coordinates in MNI-notation. NA: Not applicable; Nr.: Number of cluster, lat. = lateralization.

Table 2. _ANOVA results and descriptive statistics for brain activation by region, incentive, and activity.

Region	Effect	*F* (1,8)	*p*	η^2_p	Descriptive Statistics
Left NAcc	Incentive	0.28	.600	.001	*F*: *M* = 0.002, *SD* = 0.016
					S: *M* = 0.001, *SD* = 0.017
	Activity	14.22	<.001	.119	*A*: *M* = 0.007, *SD* = 0.016
					P: *M* = −0.004, *SD* = 0.014
	Interaction	0.80	.377	.003	
Right NAcc	Incentive	0.47	.497	.002	*F*: *M* = 0.003, *SD* = 0.024
					S: *M* = 0.005, *SD* = 0.023
	Activity	9.31	.004	.075	*A*: *M* = 0.010, *SD* = 0.023
					P: *M* = −0.003, *SD* = 0.023
	Interaction	0.72	.403	.003	
Left Insula	Incentive	0.46	.500	.002	*F*: *M* = 0.000, *SD* = 0.010
					S: *M* = 0.001, *SD* = 0.009
	Activity	10.38	**.003**	.084	*A*: *M* = 0.004, *SD* = 0.010
					P: *M* = −0.002, *SD* = 0.009
	Interaction	0.01	.934	<.001	
Right Insula	Incentive	1.14	.293	.005	*F*: *M* = 0.001, *SD* = 0.010
					S: *M* = 0.002, *SD* = 0.009
	Activity	8.44	**.006**	.065	*A*: *M* = 0.004, *SD* = 0.010
					P: *M* = −0.001, *SD* = 0.009
	Interaction	0.70	.407	.005	

NAcc = nucleus accumbens. F = financial incentive, S = social incentive, A = active risk-taking, *p* = passive risk-taking, *M* = mean, SD = standard deviation. Mean values represent parameter estimates of neural activation. Significant effects ($p < .05$) are printed in bold.

in the active condition in a large cluster encompassing larger parts of the occipital cortex and three smaller clusters: one in the bilateral dACC and right BA9, one including the left striatum, insula, inferior frontal gyrus (IFG), and the last in the right striatum. Beta estimates in the passive condition were significantly higher in three clusters located in the left hemisphere: inferior parietal lobule (IPL), middle and inferior frontal gyrus. The exact location of peaks and detailed information on the cluster extent can be found in Table 1 and Figure 4.

Contrast and conjunction analyses of risk-taking with social and financial incentives

Contrasting the data of the prior analyses on financial and social incentive types resulted in a single cluster in the right IPL (BA 39/40, see Figure 5 and Table 1).

A conjunction analysis was calculated to compare the contrasts of active and passive risk-taking of both incentive conditions. Five clusters of overlapping activation were found, located in the dACC, bilateral striatum and bilateral OC. Again, details can be found in Table 1. The findings are depicted in Figure 6.

Region of interest analyses

We conducted 2 × 2 repeated-measures ANOVAs (Incentive [financial, social] × Activity [active, passive]) with Type II sum of squares to examine activation patterns across left and right NAcc and left and right insula. Homogeneity of variance was confirmed by Levene's test for all regions (all _p_s > .72). Across all four brain regions, we found a consistent significant main effect of activity, with higher beta estimates in the active compared to passive conditions. The effect sizes ranged from small to medium ($\eta^2_p = .065$ to .119). No significant main effects of incentive or incentive × activity interactions were observed indicating that brain activity was similar across both financial and social domains. The detailed results can be found in Table 2.

Discussion

This study investigated the impact of different types of incentives on risk-taking behavior and their neural correlates. Our findings largely supported our hypotheses, confirming behavioral differences between incentive domains and identifying both domain-general and domain-specific neural networks involved in risk processing.

On the behavioral level, when incentives were social compared to financial, participants exhibited less risk-seeking behavior and took longer to respond (see Figures 2 and 3). Neuroimaging data revealed both similarities and differences across the respective incentive conditions. We identified a domain-general risk-taking network – active regardless of the incentive type, and encompassing the bilateral striatum, dorsal anterior cingulate cortex (dACC), and left insular cortex. Additionally, we found a significant difference in neural activation between conditions in the right inferior parietal lobule (IPL) with stronger activation during financial compared to social risk-taking. These data might help to advance our understanding

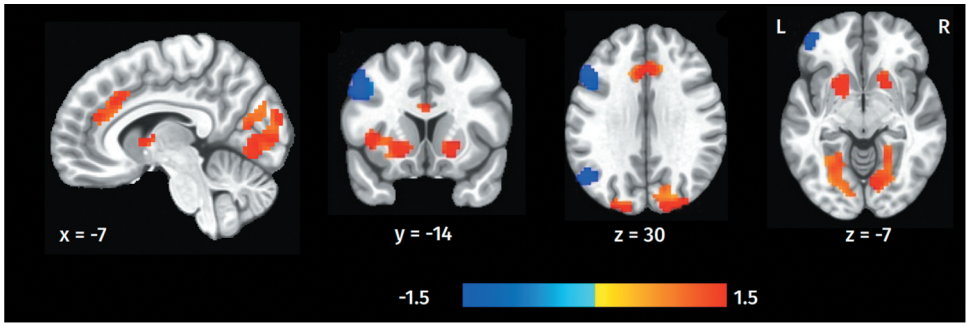

Figure 4. Activation pattern derived from contrasting within the social incentive conditions. Significant differences in beta-estimates of active > passive risk-taking within the social incentive condition, superimposed on the MNI152-2009c brain. Blue colors indicate higher activation in the passive condition, red colors indicate higher activation in the active condition.

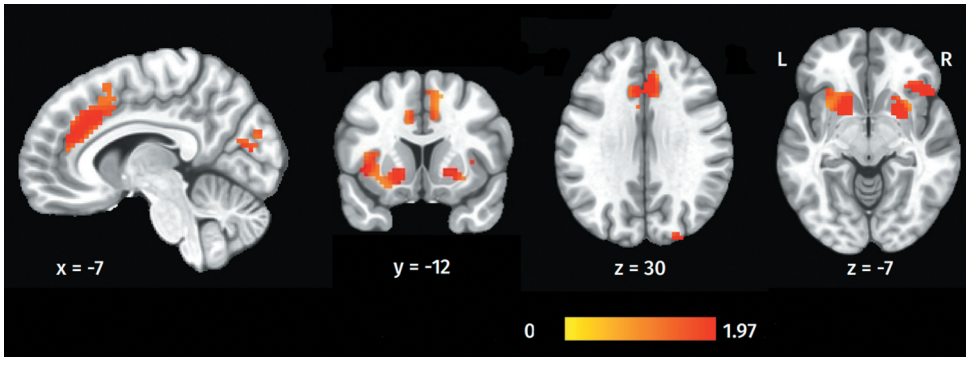

Figure 5. Activation pattern derived from contrasting the financial incentive conditions. Significant differences in beta-estimates of active > passive risk-taking within the financial incentive condition, superimposed on the MNI152-2009c brain.

of domain-general and domain-specific components of neural risk processing.

Behavioral differences between financial and social risk-taking

Participants demonstrated lower risk-taking propensity in the social incentive condition compared to the financial incentive condition, with significantly fewer balloons exploding in the social condition (35 vs 39%; $p = .001$). This data confirms our behavioral hypothesis, demonstrating that risk-taking propensity differed between incentive domains, and thus adds further data to the growing literature on domain-specific risk-taking (Blais & Weber, 2006; Sevi & Shook, 2021).

In alignment with these findings, Rosati and Hare (2016) reported significantly lower risk-taking propensity for non-financial compared to financial incentives. They

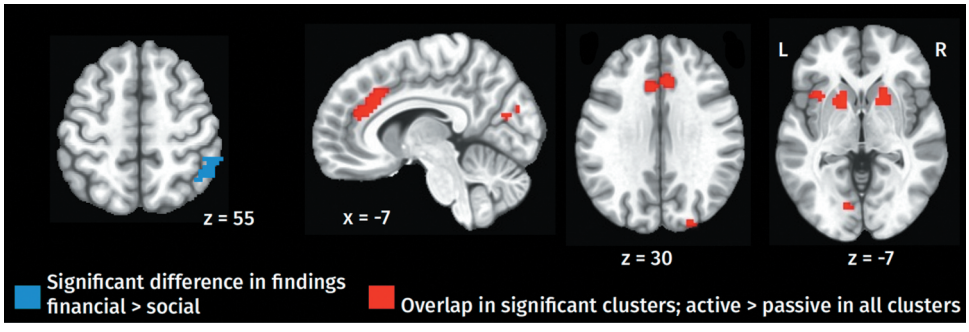

Figure 6. Contrast and conjunction comparing financial and social incentive conditions. Significant differences and commonalities of the social and financial risk-taking contrasts, superimposed on the MNI152-2009c brain.

attribute this difference to the special status of financial rewards, which enables the acquisition of other rewards, such as buying food. Similarly, von Helversen et al. (2020) found decreased sensitivity to probabilities of losses when outcomes were related to affectively rich stimuli (odors) in contrast to monetary incentives. The present findings extend this research by demonstrating that social incentives can also lead to more conservative risk-taking behavior compared to financial incentives.

A difference in decision making between the conditions is furthermore corroborated by a significant difference in response times. Participants took overall longer in the social condition.

Several explanations could account for these behavioral differences. Beyond domain-specificity, participants might have perceived the value of social rewards to be different. Furthermore, prior research shows that different heuristics are used when making decisions affecting other people (Vieider et al., 2016), potentially resulting in the here observed behavioral differences.

Type of incentives and the domain-general risk-taking network

A conjunction analysis revealed overlapping activation across incentive conditions in multiple brain regions, including the bilateral striatum, dACC, and left insular cortex. This finding largely supports one of our hypotheses, which predicted an overlap in neural activation patterns between financial and social risk-taking conditions, particularly in the dACC. However, we did not observe the hypothesized common activation in the dlPFC. This pattern of shared activation aligns with prior meta-analyses on risk-taking (Poudel et al., 2020; Wu et al., 2021), suggesting a domain-general network for risk processing being in charge regardless of the type of incentives.

The dACC was demonstrated to show consistent activation during risk-taking irrespective of incentive type. This data is in line with its role in strategy monitoring and adaptation (Kolling & O'Reilly, 2018; Kolling et al., 2016). The dACC has been extensively linked to various tasks involving cognitive control as part of the executive control network (Shenhav et al., 2013; Smith et al., 2019). Specifically, in a risk-taking context the dACC appears to monitor the current environment and signals when strategic adjustments are needed (Kolling et al., 2016), a function that, based on the present findings, seems to operate regardless of whether incentives are financial or social in nature.

Bilateral striatal activation was observed in both incentive conditions, predominantly in the caudate nucleus and extending to the nucleus accumbens. The striatum plays a well-established role in reward processing, valuation, and action selection during decision-making (Balleine et al., 2007; Lau & Glimcher, 2008; Liu et al., 2011). The finding of a striatal activation in both conditions supports the view that a common valuation network processes rewards across different domains. This finding is consistent with the common currency hypothesis (Berridge & Kringelbach, 2013), which proposes that the representation of value and motivation involves partially domain-independent neural processing.

The left insular cortex was also consistently activated across incentive conditions. The insula has been linked to affective processing during risky decisions (Clark et al., 2014; von Siebenthal et al., 2017), and lesion studies have shown that patients with insular damage demonstrate diminished sensitivity to expected value, particularly in loss domains of risk-taking (von Siebenthal et al., 2017). The consistent recruitment of the left insular cortex in the present study suggests that affective processing has to be considered a core component of risk evaluation for both incentive types.

ROI analyses demonstrated that both left and right NAcc and insular cortex showed a significant main effect (active vs. passive conditions) but no significant interactions with incentive type. This data further supports the domain-general nature of these regions in risk processing. The whole-brain analysis revealed activation in the right anterior insula (aINS) in the financial but not the social incentive condition. This apparent discrepancy likely reflects thresholding effects in the whole-brain analysis rather than a strong functional dissociation, based on the statistical comparison of both conditions in the whole brain contrast and the absence of a significant interaction in the ROI analysis.

The overlapping activation in the occipital cortex across both conditions likely reflects increased visual attention to the balloon size in active compared to passive trials. This attention-related increase in visual cortex activation has been well-documented in various studies (e.g., Green et al., 2017; Hembrook-Short et al., 2019).

The identification of a domain-general network substantiates theories proposing that risk-taking involves core neural mechanisms that operate across various contexts (Mata et al., 2018; Zhang et al., 2019). Our findings also align with research on reward anticipation,

which has identified similar domain-general networks (Gu et al., 2019), suggesting parallels between reward anticipation and risk-taking processes regarding different incentive domains.

Incentive domain-specific activation in the right IPL

The contrast between incentive conditions revealed a significant difference in neural activation pattern in the right inferior parietal lobule (IPL; BA 39/40) This finding partially supports our second hypothesis on neuronal patterns, predicting incentive domain-specific activation. However, while we hypothesized the insular cortex and NAcc as candidate regions for these differences, we instead found the primary difference in the right IPL. This unexpected finding demonstrating a stronger activation during financial compared to social risk-taking points to a specific role of the right IPL in domain-specific aspects of risk-taking.

The right IPL cluster identified in the present study predominantly encompasses the caudal (A40c) and rostrodorsal (A40rd) parts of BA40, brain areas also referred to as PFm and PFt in the Economo-Koskinas nomenclature (Caspers et al., 2013; Triarhou, 2007). Anatomically, the IPL can be divided into distinct subregions based on receptor distributions, with our present finding localized to regions spanning the rostroventral and intermediate IPL (Caspers et al., 2013). Functionally, the rostrodorsal part (A40rd) has been associated with action observation and imitation (Caspers et al., 2010; Molenberghs et al., 2009), while the caudal part (A40c) has been linked to switching between choice options (Boorman et al., 2009).

Recent work by Numssen et al. (2021) suggests that the right IPL can be functionally separated into anterior and posterior portions, with our cluster located at the border of these regions. The anterior IPL has been associated with attention shifting, while the posterior IPL is more involved in social cognition (Numssen et al., 2021). This functional division might give a hint to explain the differential activation patterns we observed between financial and social incentives, with the here identified brain area potentially representing an interface between attentional processes and social cognitive functions.

The heterogeneity in functional topography of the parietal cortex is documented in various studies (Dubois & Adolphs, 2016; Gilmore et al., 2021), also presenting substantial inter-individual variability. The right IPL forms part of the parietal memory network (PMN) (Gilmore et al., 2015), which consists of separate regions that largely differ in location between individuals (Gilmore et al., 2019, 2021). This heterogeneity may be reflected in the individual differences in risk preferences across incentive domains. Supporting this line of argumentation, Rao et al. (2018) found genetic influences on neural activation patterns in the IPL during risk-taking using a twin study design.

Several alternative explanations for the observed IPL activation differences should be considered. Rather than reflecting domain-specificity per se, this finding might indicate differences in numerical processing demands between conditions, as the IPL is also shown to be involved in numerical cognition (Park et al., 2013). Additionally, the right IPL has been shown to be involved in attentional processes (Agosta et al., 2017), and the social and financial conditions may have imposed different attentional demands. Finally, the IPL's role in the default mode network suggests that differences could reflect varying levels of self-referential processing between incentive conditions (Gilmore et al., 2019, 2021).

Taken together, our finding that right IPL activation differs between incentive conditions adds to the literature of domain-specific risk-taking. The present data suggest that while core risk processing relies on a domain-general network, brain areas linked to memory and attentional processes such as the right IPL may serve as a neural substrate for domain-specific risk preferences. Importantly, we had originally hypothesized that our ROI analyses of the insular cortex and NAcc would show domain-specific effects. However, they revealed no significant interactions between activation and incentive type, further supporting their domain-general role in risk processing.

Limitations and future research directions

Several limitations of the present study should be acknowledged. First, an inherent limitation of the BART design is that explosion probabilities must be learned by participants during task completion (Schonberg et al., 2011). Despite our efforts to minimize heterogeneity in participant characteristics that might affect learning (Mata et al., 2011), individual differences in probability learning likely influenced our data. In order to address this limitation, future studies could employ an experimental design where the probabilities are explicitly stated (such as the angling risk task; Pleskac, 2008).

Second, the expected value of balloon inflation in our design changes with balloon size, thus creating a "tipping point" where risk-taking shifts from an adaptive to a maladaptive strategy. Our parametric regressors

did not capture this qualitative difference, potentially not appropriately modeling effects related to advantageous versus disadvantageous risk-taking. Future research might specifically focus on these differences by modifying the design and analysis approach.

The financial and social conditions differ in both reward type and recipients, conflating incentive type with a self-other distinction studied previously in risk-taking (Ogawa et al., 2018; Zhang et al., 2019). Those studies keep reward type constant and describe the other as a similar individual (e.g., "another participant"), finding no response time differences (Zhang et al., 2019) or a shift toward risk-neutrality (Ogawa et al., 2018). In the present study, behavioral effects were more pronounced with significant response time differences and lower risk-taking with social incentives, suggesting a broader distinction compared to the type of recipient alone. The findings likely reflect the deliberate maximization of condition differences through qualitatively different feedback (smiley faces vs. euro amounts) and dissimilar recipients (pre-school children vs. the participant as part of the experiment) to reduce any expectation of reciprocity. Future studies could isolate these components by, for example, including a third condition where participants earn money for others.

A related concern is that the social condition may have been more ambiguous: financial rewards were communicated as exact euro amounts, whereas social rewards were indicated through less precise smiley faces. Self-reported motivation did not differ significantly between conditions, suggesting that differential engagement does not account for the behavioral differences. Instead, the less precise reward signal in the social condition may have increased deliberation demands, consistent with the observed response time differences.

Future research could disentangle these possibilities by systematically varying reward characteristics while matching perceived value across domains.

Our study included only two incentive domains, financial and social. While this experimental setup represents an important first step in comparing neural correlates across incentive types, it cannot provide a comprehensive picture of domain-general versus domain-specific neural processes. Our conclusions about domain-specificity and -generality should therefore be considered preliminary until confirmed across additional domains. Future research could address these limitations and extend the present findings in several ways. First, studies could include additional incentive domains to test the generalizability of the domain-general network and identify potential domain-specific neural correlates beyond the right IPL. An important domain to consider are health risks, as they are particularly relevant given their societal impact and, based on behavioral research, possibly discrete neural correlates (Sunstein & Zeckhauser, 2011; von Helversen et al., 2020).

Additionally, advanced methodological approaches could provide deeper insights into the neural basis of domain-specific risk preferences. Precision fMRI techniques (Gilmore et al., 2021; Gordon et al., 2017; Laumann et al., 2015) could better account for individual differences in functional topography, particularly in heteromodal regions like the IPL.

Lastly, future research might extend the present findings in several ways. The present work was conducted on a student population of young adults in Germany and is thus limited in generalizability. Future research could also investigate the clinical implications of our present findings. Excessive risk-taking is a component of several psychiatric disorders (Ashenhurst et al., 2011; Pollak et al., 2020; Reddy et al., 2014), and understanding domain-specific neural mechanisms could inform targeted interventions. This could be particularly valuable for addressing maladaptive risk behaviors in specific contexts while preserving adaptive risk-taking in others.

Conclusion

Our study reveals both domain-general and domain-specific neural correlates of risk-taking, largely supporting our hypotheses while also refining the present model by integrating some unexpected findings. The identification of a common neural network encompassing the bilateral striatum, dACC, and left insular cortex supports theories proposing domain-general mechanisms for risk processing. At the same time, the differential activation in the right IPL in financial and social incentives provides a potential neural basis for domain-specific risk preferences as observed in the prior literature.

Our findings might be a step forward in bridging the gap between behavioral evidence for domain-specific risk-taking and neuroimaging research that has primarily focused on financial incentives. This work thus highlights the importance of considering incentive type when studying risk-taking, both in laboratory settings and when translating findings to real-world contexts.

Acknowledgements

We thank Prof Dr Thorsten Fehr for his support in experimental design and analysis.

Disclosure statement

No potential conflict of interest was reported by the author(s).

Funding

The work was supported by the BMBF Neuroimaging program from the Center for Advanced Imaging (CAI) [01GO0202].

ORCID

Niels Doehring http://orcid.org/0000-0003-4858-3084

Data availability statement

The dataset generated and analyzed during the current study is available in the OpenNeuro repository: https://doi.org/10.18112/openneuro.ds007576.v1.0.0.

References

Agosta, S., Magnago, D., Tyler, S., Grossman, E., Galante, E., Ferraro, F., Mazzini, N., Miceli, G., & Battelli, L. (2017). The pivotal role of the right parietal lobe in temporal attention. *Journal of Cognitive Neuroscience*, *29*(5), 805–815. https://doi.org/10.1162/jocn_a_01086

Aklin, W. M., Lejuez, C. W., Zvolensky, M. J., Kahler, C. W., & Gwadz, M. (2005). Evaluation of behavioral measures of risk-taking propensity with inner city adolescents. *Behaviour Research and Therapy*, *43*(2), 215–228. https://doi.org/10.1016/j.brat.2003.12.007

Ashenhurst, J. R., Jentsch, J. D., & Ray, L. A. (2011). Risk-taking and alcohol use disorders symptomatology in a sample of problem drinkers. *Experimental and Clinical Psychopharmacology*, *19*(5), 361. https://doi.org/10.1037/a0024412

Balleine, B. W., Delgado, M. R., & Hikosaka, O. (2007). The role of the dorsal striatum in reward and decision-making. *The Journal of Neuroscience*, *27*(31), 8161–8165. https://doi.org/10.1523/JNEUROSCI.1554-07.2007

Berridge, K. C., & Kringelbach, M. L. (2013). Neuroscience of affect: Brain mechanisms of pleasure and displeasure. *Current Opinion in Neurobiology*, *23*(3), 294–303. https://doi.org/10.1016/j.conb.2013.01.017

Best, R., & Charness, N. (2015). Age differences in the effect of framing on risky choice: A meta-analysis. *Psychology and Aging*, *30*(3), 688. https://doi.org/10.1037/a0039447

Blais, A. R., & Weber, E. U. (2006). A domain-specific risk-taking (DOSPERT) scale for adult populations. *Judgment & Decision Making*, *1*(1), 33–47. https://doi.org/10.1017/S1930297500000334

Boorman, E. D., Behrens, T. E., Woolrich, M. W., & Rushworth, M. F. (2009). How green is the grass on the other side? Frontopolar cortex and the evidence in favor of alternative courses of action. *Neuron*, *62*(5), 733–743. https://doi.org/10.1016/j.neuron.2009.05.014

Caspers, S., Schleicher, A., Bacha-Trams, M., Palomero-Gallagher, N., Amunts, K., & Zilles, K. (2013). Organization of the human inferior parietal lobule based on receptor architectonics. *Cerebral Cortex*, *23*(3), 615–628. https://doi.org/10.1093/cercor/bhs048

Caspers, S., Zilles, K., Laird, A. R., & Eickhoff, S. B. (2010). Ale meta-analysis of action observation and imitation in the human brain. *NeuroImage*, *50*(3), 1148–1167. https://doi.org/10.1016/j.neuroimage.2009.12.112

Chandrakumar, D., Feuerriegel, D., Bode, S., Grech, M., & Keage, H. A. (2018). Event-related potentials in relation to risk-taking: A systematic review. *Frontiers in Behavioral Neuroscience*, *12*, 111. https://doi.org/10.3389/fnbeh.2018.00111

Chen, G., Taylor, P. A., & Cox, R. W. (2017). Is the statistic value all we should care about in neuroimaging? *NeuroImage*, *147*, 952–959. https://doi.org/10.1016/j.neuroimage.2016.09.066

Clairis, N., & Lopez-Persem, A. (2023). Debates on the dorsomedial prefrontal/dorsal anterior cingulate cortex: Insights for future research. *Brain*, *146*(12), 4826–4844. https://doi.org/10.1093/brain/awad263

Clark, L., Studer, B., Bruss, J., Tranel, D., & Bechara, A. (2014). Damage to insula abolishes cognitive distortions during simulated gambling. *Proceedings of the National Academy of Sciences*, *111*(16), 6098–6103. https://doi.org/10.1073/pnas.1322295111

Cox, R. W. (1996). Afni: Software for analysis and visualization of functional magnetic resonance neuroimages. *Computers and Biomedical Research*, *29*(3), 162–173. https://doi.org/10.1006/cbmr.1996.0014

Cox, R. W., & Hyde, J. S. (1997). Software tools for analysis and visualization of fMRI data. *NMR in Biomedicine: An International Journal Devoted to the Development and Application of Magnetic Resonance in Vivo*, *10*(4–5), 171–178. https://doi.org/10.1002/(SICI)1099-1492(199706/08)10:4/5<171::AID-NBM453>3.0.CO;2-L

Dubois, J., & Adolphs, R. (2016). Building a science of individual differences from fMRI. *Trends in Cognitive Sciences*, *20*(6), 425–443. https://doi.org/10.1016/j.tics.2016.03.014

Fan, L., Li, H., Zhuo, J., Zhang, Y., Wang, J., Chen, L., Yang, Z., Chu, C., Xie, S., Laird, A. R., Fox, P. T., Eickhoff, S. B., Yu, C., & Jiang, T. (2016). The human brainnetome atlas: A new brain atlas based on connectional architecture. *Cerebral Cortex*, *26*(8), 3508–3526. https://doi.org/10.1093/cercor/bhw157

Fischhoff, B., & Broomell, S. B. (2020). Judgment and decision making. *Annual Review of Psychology*, *71*(1), 331–355. https://doi.org/10.1146/annurev-psych-010419-050747

Flores, A., Münte, T. F., & Doñamayor, N. (2015). Event-related EEG responses to anticipation and delivery of monetary and social reward. *Biological Psychology*, *109*, 10–19. https://doi.org/10.1016/j.biopsycho.2015.04.005

Fonov, V., Evans, A. C., Botteron, K., Almli, C. R., McKinstry, R. C., Collins, D. L., & Brain Development Cooperative Group. (2011). Unbiased average age-appropriate atlases for pediatric studies. *NeuroImage*, *54*(1), 313–327. https://doi.org/10.1016/j.neuroimage.2010.07.033

Friedl, A., Pondorfer, A., & Schmidt, U. (2020). Gender differences in social risk taking. *Journal of Economic Psychology*, *77*, 102182. https://doi.org/10.1016/j.joep.2019.06.005

Gilmore, A. W., Nelson, S. M., Laumann, T. O., Gordon, E. M., Berg, J. J., Greene, D. J., Gratton, C., Nguyen, A. L., Ortega, M., Hoyt, C. R., Coalson, R. S., Schlaggar, B. L., Petersen, S. E., Dosenbach, N. U. F., & McDermott, K. B. (2019). High-fidelity mapping of repetition-related changes in the parietal memory network. *NeuroImage*, *199*, 427–439. https://doi.org/10.1016/j.neuroimage.2019.06.011

Gilmore, A. W., Nelson, S. M., & McDermott, K. B. (2015). A parietal memory network revealed by multiple MRI methods. *Trends in Cognitive Sciences*, *19*(9), 534–543. https://doi.org/10.1016/j.tics.2015.07.004

Gilmore, A. W., Nelson, S. M., & McDermott, K. B. (2021). Precision functional mapping of human memory systems. *Current Opinion in Behavioral Sciences*, *40*, 52–57. https://doi.org/10.1016/j.cobeha.2020.12.013

Gordon, E. M., Laumann, T. O., Gilmore, A. W., Newbold, D. J., Greene, D. J., Berg, J. J., Dosenbach, N. U., Hoyt-Drazen, C., Gratton, C., Sun, H., Hampton, J. M., Coalson, R. S., Nguyen, A. L., McDermott, K. B., Shimony, J. S., Snyder, A. Z., Schlaggar, B. L., Petersen, S. E., Nelson, S. M., & Dosenbach, N. U. F. (2017). Precision functional mapping of individual human brains. *Neuron*, *95*(4), 791–807. https://doi.org/10.1016/j.neuron.2017.07.011

Green, J. J., Boehler, C. N., Roberts, K. C., Chen, L. C., Krebs, R. M., Song, A. W., & Woldorff, M. G. (2017). Cortical and subcortical coordination of visual spatial attention revealed by simultaneous EEG-fMRI recording. *The Journal of Neuroscience*, *37*(33), 7803–7810. https://doi.org/10.1523/JNEUROSCI.0326-17.2017

Gu, R., Huang, W., Camilleri, J., Xu, P., Wei, P., Eickhoff, S. B., & Feng, C. (2019). Love is analogous to money in human brain: Coordinate-based and functional connectivity meta-analyses of social and monetary reward anticipation. *Neuroscience and Biobehavioral Reviews*, *100*, 108–128. https://doi.org/10.1016/j.neubiorev.2019.02.017

Haddad, A. D., Harrison, F., Norman, T., & Lau, J. Y. (2014). Adolescent and adult risk-taking in virtual social contexts. *Frontiers in Psychology*, *5*, 1476. https://doi.org/10.3389/fpsyg.2014.01476

Hembrook-Short, J. R., Mock, V. L., Usrey, W. M., & Briggs, F. (2019). Attention enhances the efficacy of communication in v1 local circuits. *The Journal of Neuroscience*, *39*(6), 1066–1076. https://doi.org/10.1523/JNEUROSCI.2164-18.2018

Kolling, N., & O'Reilly, J. X. (2018). State-change decisions and dorsomedial prefrontal cortex: The importance of time. *Current Opinion in Behavioral Sciences*, *22*, 152–160. https://doi.org/10.1016/j.cobeha.2018.06.017

Kolling, N., Wittmann, M. K., Behrens, T. E., Boorman, E. D., Mars, R. B., & Rushworth, M. F. (2016). Value, search, persistence and model updating in anterior cingulate cortex. *Nature Neuroscience*, *19*(10), 1280–1285. https://doi.org/10.1038/nn.4382

Kyllonen, P. C., & Zu, J. (2016). Use of response time for measuring cognitive ability. *Journal of Intelligence*, *4*(4), 14. https://doi.org/10.3390/jintelligence4040014

Lau, B., & Glimcher, P. W. (2008). Value representations in the primate striatum during matching behavior. *Neuron*, *58*(3), 451–463. https://doi.org/10.1016/j.neuron.2008.02.021

Laumann, T. O., Gordon, E. M., Adeyemo, B., Snyder, A. Z., Joo, S. J., Chen, M. Y., Petersen, S. E., McDermott, K., Nelson, S., Dosenbach, N. F., Schlaggar, B., Mumford, J., Poldrack, R., & Petersen, S. (2015). Functional system and areal organization of a highly sampled individual human brain. *Neuron*, *87*(3), 657–670. https://doi.org/10.1016/j.neuron.2015.06.037

Lei, Y., Wang, L., Chen, P., Li, Y., Han, W., Ge, M., Yang, L., Chen, S., Hu, W., Wu, X., & Yang, Z. (2017). Neural correlates of increased risk-taking propensity in sleep-deprived people along with a changing risk level. *Brain Imaging and Behavior*, *11*(6), 1910–1921. https://doi.org/10.1007/s11682-016-9658-7

Lejuez, C. W., Read, J. P., Kahler, C. W., Richards, J. B., Ramsey, S. E., Stuart, G. L., Strong, D. R., & Brown, R. A. (2002). Evaluation of a behavioral measure of risk taking: The balloon Analogue risk task (BART). *The Journal of Experimental Psychology: Applied*, *8*(2), 75–84. https://doi.org/10.1037/1076-898X.8.2.75

Liu, X., Hairston, J., Schrier, M., & Fan, J. (2011). Common and distinct networks underlying reward valence and processing stages: A meta-analysis of functional neuroimaging studies. *Neuroscience and Biobehavioral Reviews*, *35*(5), 1219–1236. https://doi.org/10.1016/j.neubiorev.2010.12.012

Mata, R., Frey, R., Richter, D., Schupp, J., & Hertwig, R. (2018). Risk preference: A view from psychology. *Journal of Economic Perspectives*, *32*(2), 155–172. https://doi.org/10.1257/jep.32.2.155

Mata, R., Josef, A. K., Samanez-Larkin, G. R., & Hertwig, R. (2011). Age differences in risky choice: A meta-analysis. *Annals of the New York Academy of Sciences*, *1235*(1), 18–19. https://doi.org/10.1111/j.1749-6632.2011.06200.x

Molenberghs, P., Cunnington, R., & Mattingley, J. B. (2009). Is the mirror neuron system involved in imitation? A short review and meta-analysis. *Neuroscience and Biobehavioral Reviews*, *33*(7), 975–980. https://doi.org/10.1016/j.neubiorev.2009.03.010

Nichols, T., Brett, M., Andersson, J., Wager, T., & Poline, J. B. (2005). Valid conjunction inference with the minimum statistic. *NeuroImage*, *25*(3), 653–660. https://doi.org/10.1016/j.neuroimage.2004.12.005

Nicolaou, N., & Shane, S. (2019). Common genetic effects on risk-taking preferences and choices. *Journal of Risk and Uncertainty*, *59*(3), 261–279. https://doi.org/10.1007/s11166-019-09316-2

Numssen, O., Bzdok, D., & Hartwigsen, G. (2021). Functional specialization within the inferior parietal lobes across cognitive domains. *Elife*, *10*. https://doi.org/10.7554/eLife.63591

Ogawa, A., Ueshima, A., Inukai, K., & Kameda, T. (2018). Deciding for others as a neutral party recruits risk-neutral perspective-taking: Model-based behavioral and fMRI experiments. *Scientific Reports*, *8*(1), 12857. https://doi.org/10.1038/s41598-018-31308-6

Park, J., Park, D. C., & Polk, T. A. (2013). Parietal functional connectivity in numerical cognition. *Cerebral Cortex*, *23*(9), 2127–2135. https://doi.org/10.1093/cercor/bhs193

Pleskac, T. J. (2008). Decision making and learning while taking sequential risks. *Journal of Experimental Psychology: Learning, Memory & Cognition*, *34*(1), 167–185. https://doi.org/10.1037/0278-7393.34.1.167

Pollak, Y., Poni, B., Gershy, N., & Aran, A. (2020). The role of parental monitoring in mediating the link between adolescent ADHD symptoms and risk-taking behavior. *Journal of Attention Disorders*, *24*(8), 1141–1147. https://doi.org/10.1177/1087054717725875

Poudel, R., Riedel, M. C., Salo, T., Flannery, J. S., Hill-Bowen, L. D., Eickhoff, S. B., Larid, A. R., & Sutherland, M. T. (2020). Common and distinct brain activity associated with risky and ambiguous decision-making. *Drug & Alcohol Dependence*, *209*, 107884. https://doi.org/10.1016/j.drugalcdep.2020.107884

Rademacher, L., Krach, S., Kohls, G., Irmak, A., Gründer, G., & Spreckelmeyer, K. N. (2010). Dissociation of neural networks for anticipation and consumption of monetary and social rewards. *Neuroimage*, *49*(4), 3276–3285. https://doi.org/10.1016/j.neuroimage.2009.10.089

Rao, H., Korczykowski, M., Pluta, J., Hoang, A., & Detre, J. A. (2008). Neural correlates of voluntary and involuntary risk taking in the human brain: An fMRI study of the balloon

analog risk task (BART). *NeuroImage*, *42*(2), 902–910. https://doi.org/10.1016/j.neuroimage.2008.05.046

Rao, L. L., Zhou, Y., Zheng, D., Yang, L. Q., & Li, S. (2018). Genetic contribution to variation in risk taking: A functional MRI twin study of the balloon analogue risk task. *Psychological Science*, *29*(10), 1679–1691. https://doi.org/10.1177/0956797618779961

R Core Team. (2021). *R: A language and environment for statistical computing*. R Foundation for Statistical Computing. https://www.R-project.org/

Reddy, L. F., Lee, J., Davis, M. C., Altshuler, L., Glahn, D. C., Miklowitz, D. J., & Green, M. F. (2014). Impulsivity and risk taking in bipolar disorder and schizophrenia. *Neuropsychopharmacology*, *39*(2), 456–463. https://doi.org/10.1038/npp.2013.218

Rosati, A. G., & Hare, B. (2016). Reward currency modulates human risk preferences. *Evolution and Human Behavior*, *37*(2), 159–168. https://doi.org/10.1016/j.evolhumbehav.2015.10.003

RStudio Team. (2016). *RStudio: Integrated development environment for R*. Posit Software, PBC. http://www.posit.co/

Saad, Z. S., Glen, D. R., Chen, G., Beauchamp, M. S., Desai, R., & Cox, R. W. (2009). A new method for improving functional-to-structural MRI alignment using local Pearson correlation. *NeuroImage*, *44*(3), 839–848. https://doi.org/10.1016/j.neuroimage.2008.09.037

Schmitz, F., Manske, K., Preckel, F., & Wilhelm, O. (2016). The multiple faces of risk-taking. *European Journal of Psychological Assessment*, *32*(1), 17–38. https://doi.org/10.1027/1015-5759/a000335

Schonberg, T., Fox, C. R., & Poldrack, R. A. (2011). Mind the gap: Bridging economic and naturalistic risk-taking with cognitive neuroscience. *Trends in Cognitive Sciences*, *15*(1), 11–19.

Sevi, B., & Shook, N. J. (2021). The relation between disgust sensitivity and risk-taking propensity: A domain specific approach. *Judgment & Decision Making*, *16*(4), 950–968. https://doi.org/10.1017/S1930297500008044

Shenhav, A., Botvinick, M. M., & Cohen, J. D. (2013). The expected value of control: An integrative theory of anterior cingulate cortex function. *Neuron*, *79*(2), 217–240. https://doi.org/10.1016/j.neuron.2013.07.007

Shou, Y., De Silva, H. S., & Olney, J. (2022). Attitudes toward ambiguous situations resemble the domain-specificity of attitudes toward risk. *Personality & Individual Differences*, *195*, 111667. https://doi.org/10.1016/j.paid.2022.111667

Skeel, R. L., Pilarski, C., Pytlak, K., & Neudecker, J. (2008). Personality and performance-based measures in the prediction of alcohol use. *Psychology of Addictive Behaviors*, *22*(3), 402. https://doi.org/10.1037/0893-164X.22.3.402

Smith, E. H., Horga, G., Yates, M. J., Mikell, C. B., Banks, G. P., Pathak, Y. J., Sheth, S. A., McKhann, G. M., Hayden, B. Y., Botvinick, M. M., & Sheth, S. A. (2019). Widespread temporal coding of cognitive control in the human prefrontal cortex. *Nature Neuroscience*, *22*(11), 1883–1891. https://doi.org/10.1038/s41593-019-0494-0

Sunstein, C. R., & Zeckhauser, R. (2011). Overreaction to fearsome risks. *Environmental & Resource Economics*, *48*(3), 435–449. https://doi.org/10.1007/s10640-010-9449-3

Theyers, A. E., Zamyadi, M., O'Reilly, M., Bartha, R., Symons, S., MacQueen, G. M., Arnott, S. R., Lerch, J. P., Anagnostou, E., Lam, R. W., Frey, B. N., Milev, R., Müller, D. J., Kennedy, S. H., Scott, C. J. M., Strother, S. C., & Arnott, S. R. (2021). Multisite comparison of MRI defacing software across multiple cohorts. *Frontiers in Psychiatry*, *12*, 617997. https://doi.org/10.3389/fpsyt.2021.617997

Triarhou, L. C. (2007). The economo-koskinas atlas revisited: Cytoarchitectonics and functional context. *Stereotactic and Functional Neurosurgery*, *85*(5), 195–203. https://doi.org/10.1159/000103258

Vieider, F. M., Villegas-Palacio, C., Martinsson, P., & Mejía, M. (2016). Risk taking for oneself and others: A structural model approach. *Economic Inquiry*, *54*(2), 879–894. https://doi.org/10.1111/ecin.12290

Voloh, B., Valiante, T. A., Everling, S., & Womelsdorf, T. (2015). Theta-gamma coordination between anterior cingulate and prefrontal cortex indexes correct attention shifts. *Proceedings of the National Academy of Sciences*, *112*(27), 8457–8462. https://doi.org/10.1073/pnas.1500438112

von Helversen, B., Coppin, G., & Scheibehenne, B. (2020). Money does not stink: Using unpleasant odors as stimulus material changes risky decision making. *Journal of Behavioral Decision Making*, *33*(5), 593–605. https://doi.org/10.1002/bdm.2178

von Siebenthal, Z., Boucher, O., Rouleau, I., Lassonde, M., Lepore, F., & Nguyen, D. K. (2017). Decision-making impairments following insular and medial temporal lobe resection for drug-resistant epilepsy. *Social Cognitive and Affective Neuroscience*, *12*(1), 128–137. https://doi.org/10.1093/scan/nsw152

Wu, S., Sun, S., Camilleri, J. A., Eickhoff, S. B., & Yu, R. (2021). Better the devil you know than the devil you don't: Neural processing of risk and ambiguity. *NeuroImage*, *236*, 118109. https://doi.org/10.1016/j.neuroimage.2021.118109

Zhang, D. C., Highhouse, S., & Nye, C. D. (2019). Development and validation of the general risk propensity scale (GRiPS). *Journal of Behavioral Decision Making*, *32*(2), 152–167. https://doi.org/10.1002/bdm.2102